# FLOW PARAMETERS IN THE INTERACTION OF TWO GAS JETS

V. D. Prikhod'ko and Yu. M. Rudov

UDC 532.522.2

On the basis of experimental data, a procedure is proposed for approximate calculation of the flow parameters at the symmetry axis in the interaction of two axisymmetric supersonic underexpanded jets of ideal gas.

The results of the present work are a continuation of the investigation of internal shock-wave structure and the distribution of the gas-dynamic parameters in parallel jets in [1], where experimental and theoretical data on the free four-nozzle gas jets were presented.

Additional experiments are undertaken on air jets with the following parameters: Mach number at the nozzle aperture $M_a$ = 1.0-3.0; degree of underexpansion $n = p_a/p_{ex}$ = 1.2-34.8; $\vartheta_a$ = 5-20; distance between nozzle centers $\bar{\ell}$ = 1.2-2.0. In the course of the experiments, shadow photographs of single-nozzle and two-nozzle jets are obtained, as well as images of the gas outflow in the plane of jet interaction by applying organic glass in the given plane before blowthrough in that plane, and the total and static pressure in the given flow regions are measured.

The distribution of the relative pressure value $p_0''$ measured by a Pitot tube (here and below, all linear dimensions are referred to the radius of the nozzle output cross section) along the symmetry axis of the two-nozzle jet is shown in Fig. 1 for three values of the relative stagnation pressure in the output cross section of the nozzle.

At some distance from the nozzle aperture, the distribution of these pressures does not depend on $N = p_0/p_{ex}$, i.e., on the degree of underexpansion. Below, this is called the section of self-similar flow. The preceding section, where the influence of the degree of underexpansion of the interacting jets is significant, is called the section of initial flow formation.

The relative pressure values measured by a Pitot tube in a single jet which is equivalent in flow rate to the two-nozzle jet is also shown in Fig. 1. On the section of self-similar flow, the relative pressure values measured by the Pitot tube in the two-nozzle jet and the equivalent single jet are practically the same. This allows the distribution of Mach numbers at the axis of the two-nozzle jet to be determined.

The relative pressure in an aggregate jet is written as follows

$$\frac{p_0''}{p_0} = \frac{p_0''}{p_0'}\frac{p_0'}{p_0} = \frac{p_{0\,\text{equiv}}''}{p_0} \tag{1}$$

where $p_0'$ is the stagnation pressure at the axis of the two-nozzle jet.

Since $p_0''/p_0'$ and $p_{0\,\text{equiv}}''/p_0$, the pressure ratio behind and in front of the discontinuity, are functions of the Mach number in the incoming flow $p_0''/p_0' = f(M)$, $p_{0\,\text{equiv}}''/p_0 = f(M')$, it follows from Eq. (1) that

$$f(M) = \frac{p_0}{p_0'} f(M'), \tag{2}$$

where M and M' are the Mach numbers at the axis of the two-nozzle jet and equivalent single jet.

The form of f is as follows [2]

$$f = \left[\frac{(\gamma+1)M^2}{(\gamma-1)M^2+2}\right]^{\frac{\gamma}{\gamma-1}} \left(\frac{2\gamma}{\gamma+1}M^2 - \frac{\gamma-1}{\gamma+1}\right)^{-\frac{1}{\gamma-1}} \tag{3}$$

Sebastopol Instrument-Making Institute. Translated from Inzhenerno-Fizicheskii Zhurnal, Vol. 56, No. 1, pp. 18-25, January, 1989. Original article submitted August 24, 1987.



0022-0841/89/5601-0012 $12.50 

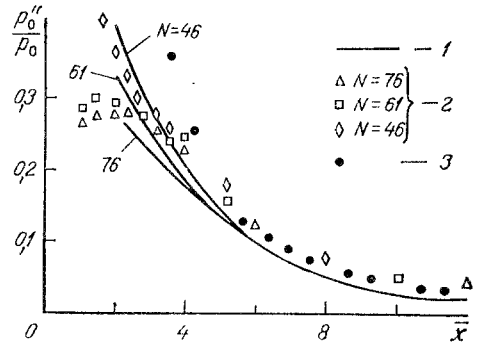


Fig. 1. Experimental and theoretical data on the total pressure at the axis of a two-nozzle jet ($M_a$ = 2.0; $\vartheta_a$ = 5°; $\gamma$ = 1.4; $\bar{\ell}$ = 1.5); 1) calculation; 2) experiment; 3) equivalent single jet.

Equation (2) gives the distribution of Mach numbers at the axis of the two-nozzle jet in the self-similar section of the flow if the stagnation pressure $p_0'$ at the axis of this jet, determined by the conditions of jet interaction, is known.

As shown by experimental data, an engineering method of calculating single-nozzle jets may be used in calculating a series of geometric and gas–dynamic characteristics in two-nozzle jets; therefore, following the results of [2, 3], the basic dependences required are given below.

The Mach jnumber $M_{ex}$ at the jet boundary and the angle of slope $\Theta_{ex}$ of the boundary at the initial point A are calculated from the formulas

$$M_{ex} = \sqrt{\frac{2}{\gamma-1}\left(N^{\frac{\gamma-1}{\gamma}}-1\right)}, \tag{4}$$

$$\Theta_{ex} = \Theta_a + \tau(M_{ex}) - \tau(M_a), \tag{5}$$

where

$$\tau(M) = \sqrt{\frac{\gamma+1}{\gamma-1}}\operatorname{arctg}\sqrt{\frac{\gamma-1}{\gamma+1}(M^2-1)} - \operatorname{arctg}\sqrt{M^2-1}.$$

The Mach number $M_B$ at point B and the abscissa $x_B$ of this point are determined by the relations for a supersonic source

$$\tau(M_B) = \tau(M_a) + 2\Theta_a, \tag{6}$$

$$x_B = \frac{1}{\sin\Theta_a}\sqrt{\frac{q(M_B)}{q(M_a)}} - \operatorname{ctg}\Theta_a, \tag{7}$$

where

$$q(M) = M\left[1+\frac{\gamma-1}{\gamma+1}(M^2-1)\right]^{-\frac{\gamma+1}{2(\gamma-1)}}.$$

The distribution of the Mach numbers over the axis in region 3 may be determined from the hypothetical-source formula [3, 4]

$$x = \left[x_B + \sqrt{\varphi}\left(\sqrt{\frac{q(M_B)}{q(M)}} - 1\right)\right], \tag{8}$$

where

$$\sqrt{\varphi} = \sqrt{\frac{2\gamma}{\gamma-1}}\Big/\Theta_{max};\quad \Theta_{max} = \Theta_a - \tau(M_a) + \frac{\pi}{2}\left(\sqrt{\frac{\gamma+1}{\gamma-1}} - 1\right).$$

The Mach number $M_3$ preceding the central discontinuity is determined from the condition that the critical pressure beyond this discontinuity is equal to the external pressure

$$N = \left(\frac{2\gamma}{\gamma+1}M_3^2 - \frac{\gamma-1}{\gamma+1}\right)^{\frac{1}{\gamma-1}}\left(\frac{1}{M_3^2}+\frac{\gamma-1}{2}\right)^{\frac{\gamma}{\gamma-1}}. \tag{9}$$

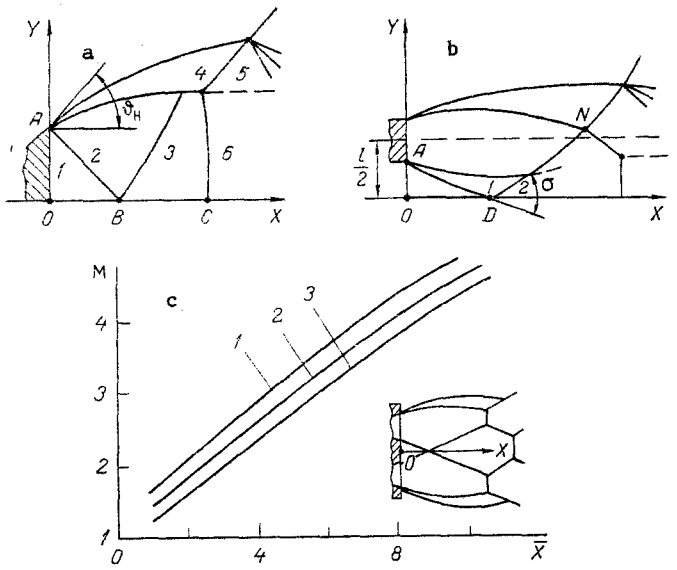


Fig. 2. Wave structure of flow and calculation of Mach numbers along the axis of the two-nozzle jet: a) single-nozzle underexpanded jet; b) two-nozzle jet in axial plane; c) calculation of Mach-number distribution along the axis of a two-nozzle jet with N = 46 (1), 61 (2), and 76 (3); $M_a$ = 2.0; $\bar{l}$ = 1.5; $\vartheta_a$ = 5°; $\gamma$ = 1.4.

Knowing the distribution of Mach numbers along the axis and the Mach number preceding the central discontinuity, its position may be determined. Good results are obtained, for example, using the Lewis–Carlson empirical formula $x_c = 1.38M_a\sqrt{(\gamma n)}$, where

$$n = N\left(1 + \frac{\gamma - 1}{2} M_a^2\right)^{-\frac{\gamma}{\gamma - 1}}$$

is the degree of underexpansion of the jet.

The triple point of the Mach configuration of discontinuities is calculated from the condition that the static pressures and angles of slope of the velocity vectors are equal at the contact discontinuity separating regions 5 and 6 (Fig. 2a). As a result, the following system of equations is obtained for determining $\delta = p_4/p_3$ as a function of $M_3$

$$\frac{\delta - 1}{\gamma M_3^2 + 1 - \delta}\sqrt{\frac{(1+\varepsilon)M_3^2}{\delta + \varepsilon} - 1} = \frac{\delta_1 - 1}{\gamma M_4^2 + 1 - \delta_1}\sqrt{\frac{(1+\varepsilon)M_4^2}{\delta_1 + \varepsilon} - 1},$$

$$\varepsilon = \frac{\gamma - 1}{\gamma + 1}, \quad \delta_1 = \frac{1}{\delta}\left(\frac{2\gamma}{\gamma + 1} M_3^2 - \frac{\gamma - 1}{\gamma + 1}\right), \tag{10}$$

$$M_4^2 = \frac{1 - \varepsilon + \varepsilon M_3^2 + M_3^2\delta - (1 - \varepsilon)\delta^2}{\delta(\varepsilon\delta + 1)}.$$

Hence determining $\delta$, the pressure $p_4$ at branching of the discontinuities is found

$$\frac{p_4}{p_{ex}} = \delta N\left(1 + \frac{\gamma - 1}{2} M_3^2\right)^{-\frac{\gamma}{\gamma - 1}}.$$

The equations of gas motion in the region of the jet boundary may be written approximately in the form [3]

$$\frac{dy}{d\Theta} = -\frac{\sin\Theta}{\nu^2 y},$$

$$\frac{dx}{d\Theta} = -\frac{\cos\Theta}{\nu^2 y}.$$

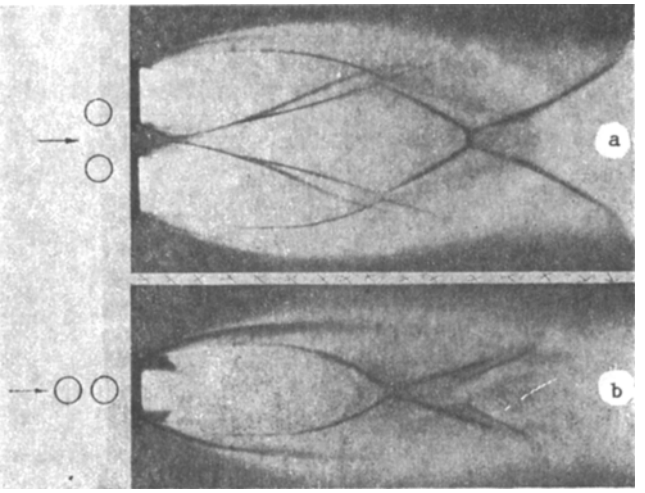


Fig. 3. Shadow recordings of two-nozzle jet in two projections ($M_a$ = 2.0; N = 46; $\bar{\ell}$ = 1.5; $\vartheta_a$ = 5°).

Integrating these equations, the equation of the jet boundary is obtained in parametric form

$$y = \sqrt{\frac{2}{\nu^2}(\cos\Theta - \cos\Theta_{ex}) + 1},$$

$$x = -\frac{1}{\nu}\int_{\Theta_{ex}}^{\Theta}\frac{\cos\Theta d\Theta}{\sqrt{2(\cos\Theta - \cos\Theta_{ex}) + \nu^2}}. \tag{11}$$

The parameter $\nu$ was defined in [2] by the formula

$$\nu^2 = \frac{2(1 - p_a/p_{ex})}{n(1 + \gamma M_a^2) - 1}.$$

Making use of the above results for a single-nozzle underexpanded jet, the interaction of two jets at the axis at point 0 is now considered (Fig. 2b). In the coordinate system DXY, the equations of the single-jet boundary are as follows

$$y = \frac{l}{2} - \sqrt{\frac{2}{\nu^2}(\cos\Theta - \cos\Theta_{ex}) + 1},$$

$$x = -\frac{1}{\nu}\int_{\Theta_{ex}}^{\Theta}\frac{\cos\Theta d\Theta}{\sqrt{2(\cos\Theta - \cos\Theta_{ex}) + \nu^2}}. \tag{12}$$

Letting y = $\ell$/2, the angle of slope of the boundary at the point of interaction (or the angle of rotation of the flow at the discontinuity which is formed at the point of interaction) is found from these equations, together with the abscissa of this point

$$\Theta_0 = \arccos\left[\left(\frac{l^2}{4} - 1\right)\frac{\nu^2}{2} + \cos\Theta_{ex}\right],$$

$$x_0 = \frac{1}{\nu}\int_{\Theta_0}^{\Theta_{ex}}\frac{\cos\Theta d\Theta}{\sqrt{2(\cos\Theta - \cos\Theta_{ex}) + \nu^2}}.$$

If the angle $\Theta_0$ is less than critical, i.e., the discontinuity is additional, the angle of slope of the discontinuity $\sigma_0$ is determined [5]

$$\sigma_0 = \operatorname{arcctg}\left[2\sqrt{c}\cos\left(\frac{\arccos dc^{-1,5} - \pi}{3}\right) - \frac{1}{3}\left(1 + \frac{\gamma + 1}{2}M_{ex}^2\right)\operatorname{tg}\Theta_0\right], \tag{13}$$

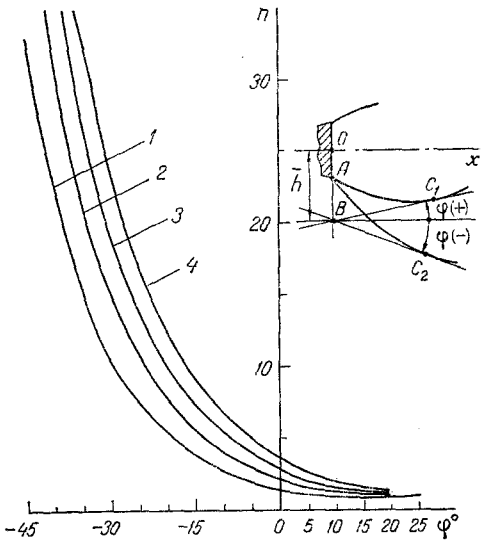


Fig. 4. Calculating the conditions of tangency of the supersonic gas jet with the plate: $M_a = 2.0$; $\gamma = 1.4$; $\vartheta_a = 5°$; $\bar{h} = 1.25$ (1), 1.5 (2), 1.75 (3), 2.0 (4).

where

$$c = \left[\frac{1}{3}\left(1 + \frac{\gamma+1}{2} M_{ex}^2\right) \operatorname{tg} \Theta_0\right]^2 - \frac{1}{3}(M_{ex}^2 - 1),$$

$$d = \left[\frac{1}{3}\left(1 + \frac{\gamma+1}{2} M_{ex}^2\right) \operatorname{tg} \Theta\right]^3 + \frac{1}{3}\left(1 + \frac{\gamma-1}{2} M_{ex}^2 + \frac{\gamma+1}{4} M_{ex}^4\right) \operatorname{tg} \Theta_0.$$

Then, from the slanting-discontinuity formulas, the Mach number and stagnation pressure behind its front are calculated

$$M_0^2 = \frac{2 + (\gamma-1) M_{ex}^2}{2\gamma M_{ex}^2 \sin^2 \sigma_0 - \gamma + 1} + \frac{2M_{ex}^2 \cos^2 \sigma_0}{(\gamma-1) M_{ex}^2 \sin^2 \sigma_0 + 2}, \tag{14}$$

$$\frac{p_0'}{p_0} = \left[\frac{(\gamma+1) M_{ex}^2 \sin^2 \sigma_0}{(\gamma-1) M_{ex}^2 \sin^2 \sigma_0 + 2}\right]^{\frac{\gamma}{\gamma-1}} \left[1 + \frac{2\gamma}{\gamma+1}(M_{ex}^2 \sin^2 \sigma_0 - 1)\right]^{-\frac{1}{\gamma-1}}. \tag{15}$$

The distribution of Mach numbers over the azis of the two-nozzle jet on the self-similar flow section is determined from the hypothetical-source formula in Eq. (4) for an equivalent single jet, taking account of the loss of stagnation pressure at the discontinuity

$$x = \sqrt{2}\left[x_B + \sqrt{\varphi}\left(\sqrt{\frac{q(M_B')}{q(M')}} - 1\right)\right], \quad f(M) = \frac{p_0}{p_0'} f(M').$$

In the section of initial flow formation, the distribution of Mach numbers is approximated by a segment of a straight line passing through the point $(x_0, M_0)$, and by the tangent to the curve $M(x)$ in the self-similar section.

The results of calculating the Mach numbers at the axis of a two-nozzle jet are shown in Fig. 2c for three values of N.

Using the theoretical values of the Mach number and stagnation pressure at the jet axis, the stagnation pressure behind a straight pressure discontinuity is determined

$$\frac{p_0''}{p_0} = \frac{p_0'}{p_0}\left[\frac{(\gamma+1) M^2}{2 + (\gamma-1) M^2}\right]^{\frac{\gamma}{\gamma-1}} \left(\frac{2\gamma}{\gamma+1} M^2 - \frac{\gamma-1}{\gamma+1}\right)^{-\frac{1}{\gamma-1}}.$$

Theoretical values of the stagnation pressure behind a straight discontinuity (continuous curves) are compared in Fig. 1 with the pressures measured by a Pitot tube. The agreement of the results may be regarded as completely satisfactory.

Having a formula for determining the Mach numbers along the axis of a two-nozzle jet, other gas-dynamic characteristics of the flow in the given region may also be calculated. This entails knowing the stagnation parameters $p_0$, $\rho_0$ behind a sloping pressure discontinuity at point 0 (Fig. 2b).

$$\frac{p_{02}}{p_{01}} = \frac{\rho_{01}}{\rho_{02}} = \left\{\left(\frac{2\gamma}{\gamma+1} M^2 \sin^2\sigma - \frac{\gamma-1}{\gamma+1}\right)^{\frac{1}{\gamma-1}} \left[\frac{2}{\gamma+1}\left(\frac{1}{M_{ex}^2 \sin^2\sigma} + \frac{\gamma-1}{2}\right)\right]^{\frac{\gamma}{\gamma-1}}\right\}^{-1}, \quad (16)$$

where $\sigma$ is the angle of slope of shock wave ON to the direction of the boundary streamline at point 0.

In deriving the formula for the temperature distribution $T_i = f(x)$, the energy transformation at discontinuities must be taken into account. Since the total energy of the flow is unchanged on passing through the discontinuity, the following expressions are obtained for the enthalpy $h_0 = c_p T_0 = \gamma/(\gamma - 1)\ p_0/\rho_0$ and the temperature of the stagnation flow: $h_{01} = h_{02} = h_0$, $T_{01} = T_{02} = T_0$.

Now using the formulas for the isentropic flow

$$p_i = p_{02}\left(1 + \frac{\gamma-1}{2} M_i^2\right)^{\frac{\gamma}{1-\gamma}},$$

$$\rho_i = \rho_{02}\left(1 + \frac{\gamma-1}{2} M_i^2\right)^{\frac{1}{1-\gamma}},$$

$$T_i = T_0\left(1 + \frac{\gamma-1}{2} M_i^2\right)^{-1},$$

in which subscript i denotes the parameter values at an arbitrary point on the axis OX behind point D. The position of point D is determined by combined solution of the equations of the boundary of the single jet and the axis OX.

Shadow recordings of a two-nozzle jet in two projections are shown in Fig. 3. The initial outflow parameters correspond to the conditions investigated here. The photographs give additional information on the shock-wave structure, the boundaries of the jet in the characteristic cross sections, and the dimensions of the regions in which the gas-dynamic parameters were determined above.

The results obtained on the gas-dynamic parameters in the symmetry plane of parallel two-nozzle jets may also be used in calculating nonparallel gas jets, whose axes either intersect or diverge. It is evident that, in the latter case, interaction of the jets demands a larger initial total pressure $p_0$ than in the case of parallel or converging jets.

It is of interest to determine the influence of the angle of divergence of the jets on the gas dynamics of their interaction. To this end, as shown in Fig. 4, the nozzle is fixed with its center at point 0, and at a distance h = 0B a plane which may be rotated relative to point B is established. The angle $\phi$ with the axis OX may be regarded as positive in counterclockwise rotation and negative in clockwise rotation. For each angle $\phi$, there is a definite value of the degree of underexpansion of the jet at which the jet boundary touches the plate. Knowing these values of the underexpansion, the required initial interaction parameters of two-nozzle jets may be established (the angle $\phi$ is positive for converging jets and negative for diverging jets). It is clear that, in investigating two-nozzle jets, the lines $BC_1$ or $BC_2$ are their axes.

The results of calculating the initial stage of interaction of two-nozzle jets are shown in Fig. 4. Four values of $\bar{h}$ – a characteristic similar to the nozzle dispersion $\ell$ considered above – are chosen in the course of the calculations.

The calculations show that, for a diverging jet ($\phi < 0$), considerable underexpansion is required if interaction of the jet at the axis is to occur.

Note that, when $n > n_*$, reverse gas flows in the direction of the nozzles begin to form; the investigation of such flows is a separate problem, of great practical importance.

## NOTATION

M, Mach number; n, degree of underexpansion of jet; p, $\rho$, T, pressure, density, temperature; $\gamma$, adiabatic index; $\vartheta_a$, semivertex angle of nozzle; $\Theta$, angle of rotation flow; $\ell$, dis-

tance between nozzle axes; $\tau(M)$, $q(M)$, $\pi(M)$, gas-dynamic functions; $\delta$, pressure drop at shock wave; $\sigma$, angle of slope of shock wave.

## LITERATURE CITED


1. Yu. M. Rudov and V. N. Uskov, Inzh.-Fiz. Zh., 22, No. 6, 1133 (1972).
2. I. P. Ginzburg, Aerogas Dynamics [in Russian], Moscow (1966).
3. I. P. Ginzburg, B. N. Sokolov, and G. A. Akimov, in: Gas Dynamics and Heat Transfer [in Russian], Vol. 2, Leningrad (1970), pp. 38-55.
4. V. G. Dulov and G. A. Luk'yanov, Gas Dynamics of Emission Processes [in Russian], Novosibirsk (1984).
5. G. M. Arutyunyan and L. V. Karchevskii, Reflected Shock Waves [in Russian], Moscow (1973).


# QUESTION OF THE MOTION OF A SYSTEM OF SEQUENTIAL COAXIAL VORTEX RINGS IN A HOMOGENEOUS FLUID


O. G. Martynenko, I. A. Vatutin, N. I. Lemesh, and P. P. Khramtsov



UDC 532.516



Results are presented of an experimental investigation of the singularities of the motion of a system of interacting toroidal vortices in a homogeneous fluid.


In connection with the possibility of a practical application of ring vortices to remove smoke, harmful gases, etc. in industrial plants, numerous theoretical and experimental investigations have recently been performed concerning the mechanism of ring vortex formation and the regularities of their propagation in gases and liquids [1-4]. Significantly less attention has been paid to questions of propagation of a system of coaxial vortex rings following one another. Meanwhile a number of specific properties of the motion is of interest in these cases.

It is known [5] that there is a complete analogy between the equations of vortical fluid motion and the fundamental equations of the theory of electromagnetism. Moreover, a relationship is obtained that describes toroidal vortex interaction that is analogous to the Biot-Savart law about the action of an electrical current on a magnetic pole. This would permit a general representation to be obtained about the dynamics of the motion of two coaxial vortex rings with identical direction of rotation.

Their mutual influence is that the radius of the vortex going forward increases while that of the following vortex diminishes. While the radius of the first vortex is made greater than the radius of the second, its motion is retarded and that of its follower is accelerated.

An experimental verification of the "leapfrogging" of two vortex rings was obtained in [6, 7]. We take the following notation $2,1 \rightarrow 1,2 \rightarrow 2,1$ for convenience in describing the "leapfrogging" to two vortex rings.

Denoting by 1, 2, 3 the first, the next, and the last vortices, respectively, from the exit of a vortex generator and taking account of what was said above, we can give a basis for the following possible variants of the "leapfrogging" of three coaxial vortex rings: 1) $3,2,1 \rightarrow 3,1,2 \rightarrow 1,3,2 \rightarrow 1,2,3 \rightarrow 2,1,3 \rightarrow 2,3,1 \rightarrow 3,2,1$; 2) $3,2,1 \rightarrow 1,2,3 \rightarrow 3,2,1$; 3) $3,2,1 \rightarrow 1,2,3 \rightarrow 2,1,3 \rightarrow 2,3,1 \rightarrow 3,2,1$; 4) $3,2,1 \rightarrow 1,2,3 \rightarrow 1,3,2 \rightarrow 3,1,2 \rightarrow 3,2,1$. It is assumed here that the vortex ring of large radius does not overtake the ring of smaller radius and that two kinds of interaction, doubling (merger of two vortices) and tripling (merger of three vortices) can occur.

If the number of vortex rings is $N > 3$ then the quantity of possible interactions naturally grows. For favorable relationships between the sizes, intensity, and repetition rate


A. V. Lykov Institute of Heat and Mass Transfer, Academy of Sciences of the Belorussian SSR, Minsk.


Translated from Inzhenerno-Fizicheskii Zhurnal, Vol. 56, No. 1, pp. 26-28, January, 1989. Original article submitted December 8, 1987.




0022-0841/89/5601-0018$12.50